

Geometry and Roughness Effect at the RCC Interface-Earth Dam Causing Leakage in Mae Suai Composite Dam, Thailand

S. Soralump¹, K. Wannasiri², and S. Prempramote³

¹Geotechnical Engineering Research and Development Center, Civil Engineering Department, Kasetsart University, Thailand

²PhD. Candidate, Department of Civil Engineering, Faculty of Engineering, Kasetsart University, Thailand

³Department of Civil Engineering, Faculty of Engineering, Kasetsart University, Thailand

E-mail: soralump_s@yahoo.com

ABSTRACT: Mae Suai Dam is an earth zone dam with RCC section in the center of downstream slope located at Mae Suai district, Chiang Rai, Thailand. The differential settlement at the joint between RCC spillway and the earth-filled section caused leakage near the crest of the dam. This unusual settlement is the result of a joint where materials of different stiffness are connected; the settlement pattern depends on the shape and interface shear strength of the contact area. In this paper, non-uniform settlement of Mae Suai Dam was investigated by 2D & 3D FEM using MIDAS GTS for Fully Coupled Stress-Seepage analyses. The results of finite element analyses were verified with the geodetic measurements data and observation in rehabilitation processes of Mae Suai Dam. Roughness and taper effects were studied by analyzing the settlement along the dam crest using 2D FEM analysis by varying the interface stiffness between the earth dam and RCC spillway to characterize the settlement of each condition and verified with the geodetic measurements. The analysis revealed that the effect of roughness and taper resulted in non-uniform. If these types of dam structures are selected in other projects, the pattern of settlement should be considered in accordance with the guidelines for dam crest design to prevent damage and leakage caused by the non-uniform settlement of the dam.

KEYWORDS: Composite dam, Differential settlement, Finite element analysis, and Taper effect.

1. INTRODUCTION

Selection of dam types are based on the availability of construction materials, geological conditions of the dam, propose of the dam along with economic and environment factors. Therefore, various types of dams, including earth dam, zoned dam, concrete dam, rock-fill dam, and composite dam are constructed based on these factors (USBR, 2011, Panthi and Soralump, 2020, Soralump et al., 2021b). A composite dam is the combination of one or more dam types (Alidadi and Hakami, 2014, Jia et al., 2018). A geological structure and site condition mainly leads to the construction of composite dam. It is built on the site, satisfying different foundation conditions. The composite dam is composed of two different materials, and the interface between those materials have a stiffness difference that could lead to a significant problem (Dong Soo, 2018). Non-uniform settlement along the earth-concrete interface is one of the potential problems in composite dam (Chang and Oncul, 2000).

Mae Suai Dam is an earth zone dam with RCC (Roller Compacted Concrete) section in the center of downstream slope located at Mae Suai district, Chiang Rai, Thailand, as shown in Figure 1. The differential settlement at the joint between RCC spillway and the earth-filled section caused leakage near the crest of the dam (Soralump et al., 2016). This unusual settlement is the result of a joint where materials of different stiffness are connected; the settlement pattern depends on the shape and interface shear strength of the contact area. The surface roughness is found to have a substantial effect on the interfacial shear strength and shear behavior, with the shear strength increasing with increased surface roughness level (Chen et al., 2015, Wang et al., 2020)

Finite Element Method (FEM) is widely used nowadays for its ability to model complex geometries, peculiar geological conditions, and a variety of boundary conditions (Soralump et al., 2019, Soralump et al., 2021a). Many researchers have investigated the settlement behavior of dams by FEM analysis and verified with the geodetic measurements in previous 2 decades. Foster et al. describes the results of a statistical analysis of failures and accidents of embankment dams, specifically concentrating on those incidents involving piping and slope instability by comparing the characteristics of the dams which have experienced failures and accidents to those of the population of dams (Foster et al., 2000). Lollino et al. presents a case history for the construction of the Pappadai rock-fill dam in Italy, 2D plane-strain finite element

analyses were performed to reproduce the soil-structure interaction so that the effects of reservoir impoundment (Lollino et al., 2005). The process of water infiltration into the originally unsaturated rock-fill dam (Gouhou Dam) has been studied using three-dimensional saturated-unsaturated seepage theory (Chen and Zhang, 2006). Gikas and Sakellariou have studied the long-term (>30 years) settlement behavior of the Mornos dam on the basis of finite element analysis and vertical displacement data, compares actually measured deformations resulting from a continuous geodetic monitoring record of the dam behavior with a numerical back analysis (Gikas and Sakellariou, 2008). Farias et al. presents a methodology for advanced numerical analysis of earth dams, considering all design stages (Farias and Cordão Neto, 2010). It also includes transient analysis of safety factors and can be applied to general three-dimensional conditions, considering unsaturated materials and the interrelation between hydraulic and mechanical phenomena by simultaneously solving equilibrium and continuity conditions. Mahinroosta et al. presents a new collapse prediction framework involving an introduction of a stress dependent collapse coefficient which is directly obtained from results of triaxial tests (Mahinroosta et al., 2015). Two prediction methods for post-construction settlement of CFRDs (Concrete face rock-fill dams) was presented by Kermani et al. (Kermani et al., 2016). In the first method, post-construction settlements are estimated using height of the embankment. In the second method, characterization of the stress-strain behavior of the compacted rock-fill layers during construction allows prediction of the subsequent stress-strain-time behavior of the embankment. The behavior of Gavoshan dam was evaluated during construction and the first impounding (Rashidi and Haeri, 2017). A two-dimensional numerical analysis was conducted based on a finite difference method on the largest cross-section of the dam using the results of instrument measurements and back analysis. The vertical and lateral displacements of an earth dam in Guangxi Province, southwestern China, were monitored over an 18-year period (Luo et al., 2019). The effect of concrete slab-cushion layer interface on the performance of face slabs in concrete face rock-fill dams is investigated using the finite element method (Saber et al., 2018). 3D Nonlinear Analysis of Atatürk Clay Core Rock-fill Dam were examined by effects of the various reservoir water heights and confirmed by the geodetic measurements (Kartal et al., 2019). The mechanical behavior of Shirin-Dare Dam was evaluated at the end of construction, initial impounding, and operation time through using the results of

instruments and numerical analysis conducted by FLAC software (Rashidi and Haeri, 2017). An analysis of the permanent deformation was observed in the core of a rock-fill dam (Pérez-González et al., 2020). Stress conditions that may be associated with a rapid accumulation of permanent deformation were identified, and an analysis method is proposed to specify the acceptable heavy traffic conditions for the dams.

The settlement of dam was analyzed based on the instrumentation data by the past 30 years by Soralum and Thongthamchart with various prediction methods to find out that the clay core and rock-fill material shows secondary compression behavior (Soralump et al., 2009). The dam settlement is close to the calculated total settlement, including the creep effect. However, the lack of available literature exists in terms of the effect of roughness and taper of the contact area between the earth dam and RCC section that affects the settlement pattern of the composite dam.

In this paper, non-uniform settlement of Mae Suai Dam was investigated by 2D & 3D FEM using MIDAS GTS for Fully-Coupled Stress-Seepage analyses. The results of finite element analyses were verified with the geodetic measurements data and observation in rehabilitation processes of Mae Suai Dam. Roughness and taper effects were studied by analyzing the settlement along the dam crest using 2D FEM analysis by varying the interface stiffness between the earth dam and RCC spillway to characterize the settlement of each condition and verified with the geodetic measurements.

2. CHARACTERISTICS OF MAE SUAI DAM

Mae Suai Dam is a 59 m high structure with 400 m crest length and having a reservoir capacity of 73 million cubic meters (Figure 1). The dam has been in operation since 2003. The RCC section is used as an overflow spillway and was designed for 500 years return period of the flood. The RCC material is a low-paste RCC covered with conventional concrete (CVC). Figure 2 shows the longitudinal and transverse sections of the dam. The RCC structure is laid upon sound rock foundation. Sandy material in the riverbed has been removed to prevent the under seepage and potential soil liquefaction. The RCC section consists of an overflow spillway and gravity retaining wall at both sides to create flow channels and retain the earth dam at both sides (Figure 3).



Figure 1 Mae Suai Dam

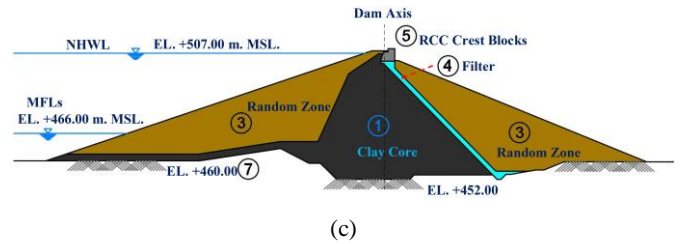
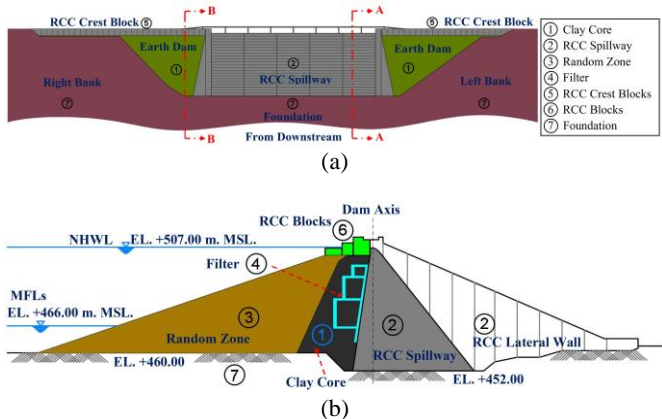


Figure 2 Longitudinal and Cross Section of Mae Suai Dam : (a) Longitudinal section; (b) Cross section A-A; (c) Cross section B-B

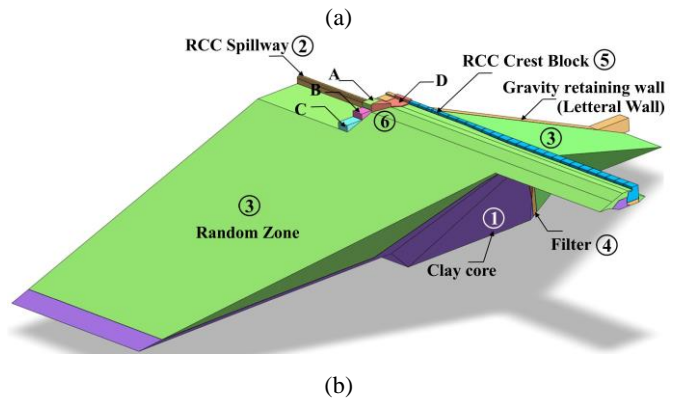
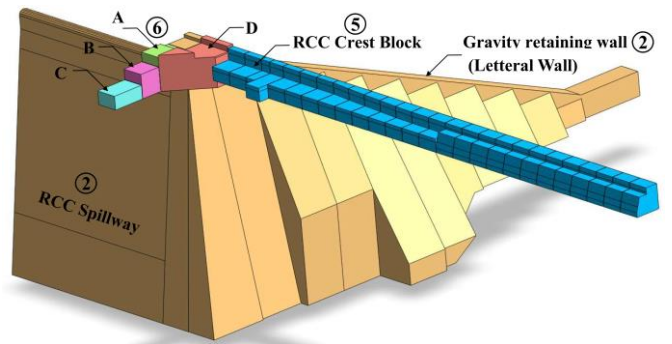


Figure 3 Component of Mae Suai Dam : (a) RCC spillway section and gravity retaining wall; (b) Earth dam section and RCC Block

The RCC section is surrounded by earth zone dam. Core trench of the earth zone dam was excavated to the foundation rock in the riverbed and abutments. Impervious core or clay core could be categorized as a low-plasticity clay (CL) and clayey sand (SC) materials consists of internal filter (sand and gravel) to reduce the water pressure and discharge the seepage water into RCC gallery. Shell zone or random zone is made up of semi-impervious coarse grain earth (low-plasticity clay (CL), clayey sand (SC) and silty sand (SM)) with horizontal drain to drain out the water during drawdown period and maintain the stability of shell zone. The earth zone extends on both sides of the abutment. The 6 m high RCC retaining block was constructed over the earth-filled material at the downstream of dam crest to reduce the earth-fill work on downstream slope and lower the construction cost. The transition trapezoidal RCC block (Block D) was constructed near the joint between RCC spillway section and earth zone dam. Furthermore, to prevent the erosion at the crest of earth dam during the overtopping of spillway, RCC blocks A, B and C were constructed as a water guide wall (wing wall) as shown in Figure 3 and Figure 4. These blocks were placed directly over the earth filled material.



Figure 4 Spillway wing wall and Location of Surface Monument (Photo by RID)

In 2004, after 1 year of operation of Mae Suai Dam, water overflowed the spillway, and leakage was observed at the downstream crest in contact area between earth fill dam and RCC spillway structure. The water flow was clearly observed behind the RCC block, where differential settlement was also clearly visible (Figure 5). The leakage was observed when reservoir reached a certain elevation near the dam crest. The maximum flow rate observed was 1.5 cubic meters per minute with the approximated water head of 1.2 m. The different settlement was extrapolated to be the cause of the leak. The repair work has been done by installing the impervious membrane over the surface of RCC blocks. The leakage flow was reduced after the repair of dam but did not disappear completely (Soralump et al., 2016).



Figure 5 Leakage observed at the joint between RCC and earth fill dam; the differential settlement is clearly seen (Photo by RID)

3. GEODETIC MEASUREMENT DATA AND OBSERVATION

Dam behavior during its construction and operation is an indicator of dam safety. Several instruments, i.e., piezometer, inclinometer, relief well, joint meter, surface monument (SM) & benchmark, thermocouple, seepage flowmeter, pendulum, etc., were installed in the dam body during its construction and operation phase. Vertical displacement along the dam crest was recorded from the surface monument every year since 2003. The measured settlement at each surface monument from 2003 to 2014 is as shown in Figure 6. The maximum settlement was observed near the interface between spillway and earth fill dam section (SM-3 and SM-6) and decreases gradually as it moved near the abutment. The settlement in earth fill section was, however, greater than the RCC section. The settlement at SM-3 and SM-6 were 1.12 % and 1.19%, respectively, and were both greater than 1% which is a typical settlement of a standard of earth fill dam (USBR, 2011). Likewise, the spillway section has a very low settlement, i.e., approximately 0.18% of the dam height.



Figure 6 The settlement of the RCC section and earth fill (2014)



Figure 7 Elevation of RCC Block D and differential settlement at left bank (Photo by RID)

The differential settlement between RCC spillway and earth dam section can be observed prominently in the contact of two sections from the outside. The designer had the intention to deal with future differential settlement by making the crest elevation of earth dam section to be higher than the RCC spillway section, RCC Block D is, therefore higher than the spillway section, as shown in Figure 7. However, RCC Block D appeared to be raised over the adjacent RCC spillway with the passage of time, and therefore higher differential settlement is observed at this section (Figure 7 and Figure 8). The differential settlement of the dam had started after the first year of its operation in 2003.



Figure 8 The settlement of the earth fill (Photo by RID): (a) 2003; (b) 2004

Figure 9 shows the location of observation points used to measure the settlement of RCC Block A, B, and C (Guide Wall). The vertical displacement of these RCC blocks on the right side of the dam is as shown in Figure 10. The maximum settlement was measured at the end of Block C, while Block A, that was adjacent to the spillway, had the lowest settlement. The location of block A represents the rotation of RCC block, and therefore the crack was observed at the contact between Block A, Block D, and RCC Spillway (Figure 11 and Figure 12). Since the leakage was also observed in the contact area, the repair work was done in 2005 by removing the precast concrete panels that covered RCC Block D and installing the impervious membrane over the surface of RCC blocks along with grouting in the cracks between RCC Block A, B, C and RCC spillway. The leakage flow was reduced after the repair work, but some leakage still persisted. Sub-drain system for filtering and collecting the leakage water was then installed at the downstream toe of RCC crest block and RCC block D to prevent unnecessary seepage. However, it was found that the crack expanded with the passage of time, and the rate of leakage increased significantly each year, indicating the risk of suffused flow that might lead to piping failure.



Figure 9 Reference point at surface of RCC block (Photo by RID)

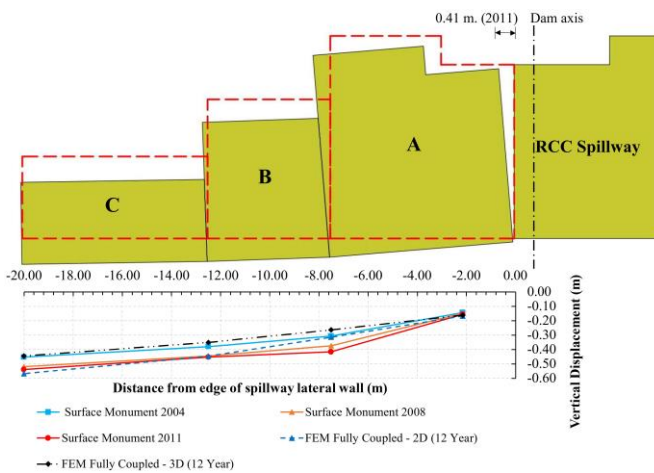


Figure 10 Vertical displacement and deformation of RCC Block A, B, C

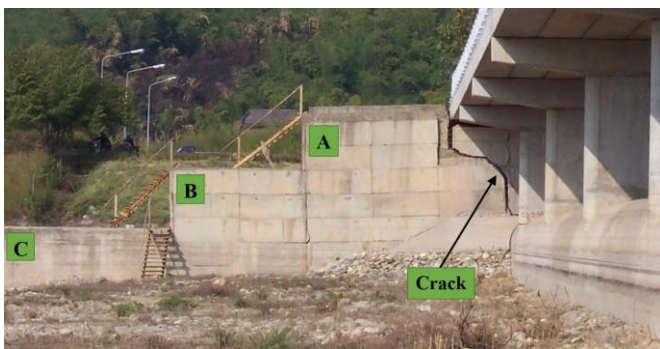


Figure 11 Crack between RCC spillway and Block A (Photo by RID, 2005)

4. 2D AND 3D FINITE ELEMENT MODEL OF MAE SUAI DAM

The finite element analyses were performed using a geotechnical analysis software MIDAS GTS. In this research, 2D and 3D finite element model of Mae Suai Dam was created according to the original dam geometry. Mohr-Coulomb model was used for the foundation, filters, and RCC materials, while Modified Cam-clay model was used for random and core of the dam. Fully coupled Stress-Seepage was used in the analyses; it was a two-way coupled analysis between seepage analysis and stress analysis. Both analyses are used to solve the coupled equation (MidasGTS, 2018).



Figure 12 Crack in RCC Block D (Photo by RID, 2005)

In both 2D and 3D FEM, transient seepage analysis was performed, the function of water level change was determined from the water retention record in the first 3 years. The water level on the upstream side was varied from the Minimum Water Level (MFLs) to the Normal High-Water Level (NHWL) (Figure 2). Gravity loads and Steady-state seepage were the initial conditions; the water level was set to the MFLs. During the first fill of a reservoir, the water level was increased from MFLs to NHWL within 1 year, and other years the water level fluctuated during the period of storage in 1 year. Likewise, total of 12 construction stages (1 year/stage) with time step of one month was used in analysis based on geodetic monitoring data.

4.1 Constitutive Model

4.1.1 Mohr-Coulomb Material Model

The Mohr-Coulomb model is used to simulate most terrain as it displays sufficiently reliable results for general nonlinear analysis of the ground. The model states that failure occurs when the shear stress τ and the effective normal stress σ_n acting on any element in the material satisfy the following linear equation 1.

$$|\tau| = c - \sigma_n \tan \phi \quad (1)$$

Where c and ϕ are the cohesion and the internal friction angle. The equation 1 shows that failure occurs at the stress state where the largest Mohr circle comes across the Coulomb friction failure envelope. It also shows that the intermediate principal stress σ_2 ($\sigma_1 \geq \sigma_2 \geq \sigma_3$) does not have an effect on the failure condition. Hence, the yield function of the Mohr-Coulomb failure plane is as shown in equation 2.

$$f = |\tau| + \sigma_n \tan \phi - c = 0 \quad (2)$$

Expressing the Mohr-Coulomb criterion using principal stress terms ($\sigma_1 \geq \sigma_2 \geq \sigma_3$), equation 2 can be rearranged into the following equation 3 & 4.

$$\frac{\sigma_1 - \sigma_3}{2} = -\frac{\sigma_1 - \sigma_3}{2} \sin \phi + c \cos \phi \quad (3)$$

$$\sigma_1 \frac{1 + \sin \phi}{2c \cos \phi} - \sigma_3 \frac{1 - \sin \phi}{2c \cos \phi} = 1 \quad (4)$$

4.1.2 Modified Cam-clay Material Model

The Modified Cam-clay model provided in GTS is also based on the elastic-plastic hardening theory. Formulation of the Modified Cam-clay model in GTS uses all effective stresses and is materialized using nonlinear elastic and the implicit backward Euler method (Borja, 1989).

Nonlinear elastic behavior represents the increase in bulk modulus when pressure is applied to the material. Also, the associated flow rule is used, and the failure surface can increase or decrease depending on hardening/softening behavior (MidasGTS, 2018). Figure 13a displays the relationship between the ground volume change and hydrostatic pressure using the normal consolidation line and overconsolidation line, or swelling line. If the stress increases and surpasses the hydrostatic pressure, the volume change follows the overconsolidation line. If the increase in hydrostatic pressure is enough, the volume change passes through the intersection of the normal and overconsolidated lines and follows the normal consolidation line. M is defined as the slope of the critical state line in Figure 13 projected onto the p' - q plane, as shown in Figure 13b.

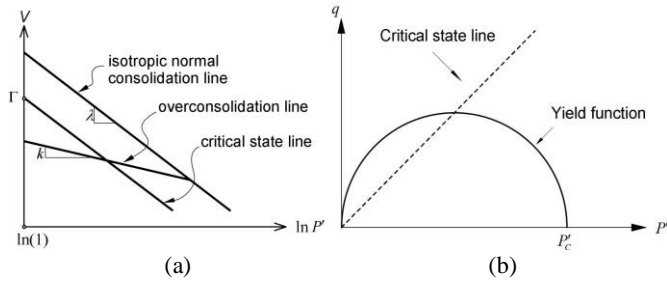


Figure 13 Critical state line (MidasGTS, 2018): (a) Pressure and specific volume relationship; (b) Yield function of Modified Cam-clay model

The material properties of the ground are generally obtained from 1D consolidation experiments. The compression index C_c and recompression index C_s are generally obtained from the void ratio, e , and $\log_{10}(P)$ graph. The compression index and recompression index are as shown in equations 5 & 6, respectively, using the slope of normal consolidation line λ and slope of overconsolidation line k .

$$\lambda = \frac{C_c}{2.303} \quad (5)$$

$$k = \frac{C_s}{2.303} \quad (6)$$

The slope of the critical state line M can be estimated from the relationship with the effective shear resistance angle.

$$M = \frac{6 \sin \phi}{3 - \sin \phi} \quad (7)$$

Likewise, Γ can be calculated using equation 8, after the specific volume N of the normal consolidation line at $p = 1.0$ as shown in Figure 13a.

$$\Gamma = N - (\lambda - k) \ln 2 \quad (8)$$

The overconsolidation ratio (OCR) is defined using equation 9, where p'_{max} is the maximum effective hydrostatic pressure on the material, and p'_v is the initial effective hydrostatic pressure.

$$OCR = \frac{p'_{max}}{p'_v} \quad (9)$$

4.2 Geometry Model

2D finite element model was performed under plane-strain conditions. A total of four cross-sections with the varying earth dam section and foundation depth at the right bank were taken into consideration as shown in Figure 14. To avoid the boundary effects caused by the constraints of the numerical model in section 4.4, the foundation of the upstream and downstream embankments has been extended 120 m in both directions, twice the maximum height of the dam (Gikas and Sakellariou, 2008). Therefore, the deformation of the dam body had very little impact due to the constraints of the model.

The plain-strain triangular element type was used in RCC and soil element with three nodes.

Element sizes varies from 1 m to 20 m; the smaller element size is located at the top of the dam and increases when its lowered. At the dam crest, where the type of construction joint is specified and needs more accuracies to measure the settlement value, smaller elements are defined. The contact surface between RCC Spillway and Block A, B & C are defined as construction joints because each part can slide and separate. Therefore, to transfer the compression, rigid link-type interface elements have been used. The rigid link was a high stiffness element that is only able to transfer compressive forces in a horizontal direction, and the movement of side surface was allowed in vertical direction.

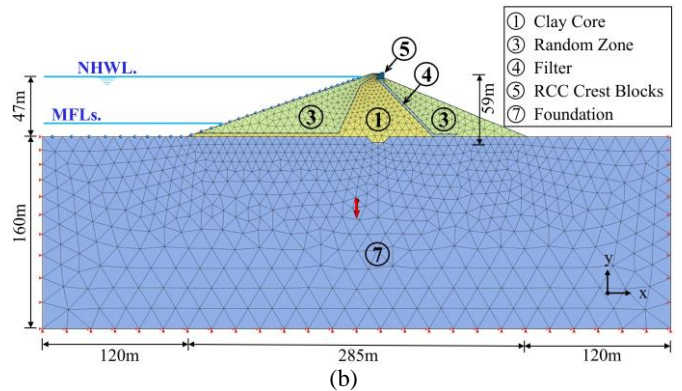
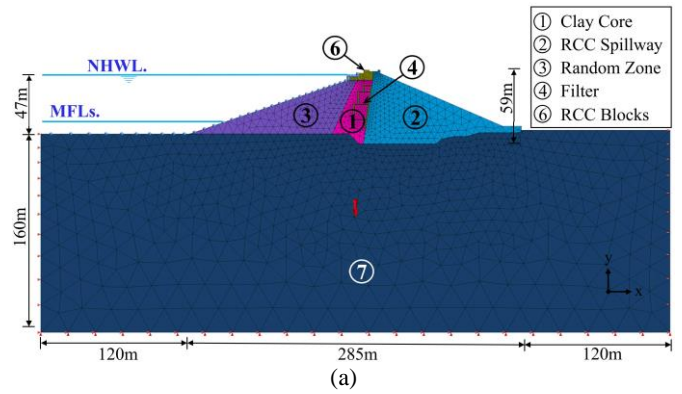


Figure 14 2D Finite Element Model of Mae Suai Dam: (a) 59.00 m high (Spillway Section); 57.50 m high (Earth Dam Section)

The magnitude of the vertical displacement at each position of SM having different foundation depths were determined using 2D finite element analysis and was verified using geodetic monitoring data. However, the vertical displacement along the dam crest could not be clearly demonstrated because the shape of the foundation was trapezoidal. Furthermore, the contact area of earth dam section with the RCC spillway and lateral wall were unregulated, i.e., the RCC Spillway slopes downward as a counterweight of the lateral wall, and therefore, the effect of shear interface of the contact area could not be considered. Therefore, 3D Finite Element Model was used in Mae Suai Dam to account these problems (Figure 15). The upstream, downstream, left, and right embankments extend more than twice of the maximum height of the dam. Likewise, the depth of the foundation was similar to that of the dam height to avoid boundary effects (Kartal et al., 2019). Solid elements, i.e., linear 4-node tetrahedron elements, were used in 3D FEM. Element sizes varies from 1m to 20m; the smaller element size is located at the top of the dam crest and increases when its lowered. The RCC spillway, RCC crest block, RCC block A, B, and C were connected with rigid link element that can only transfer the compression.

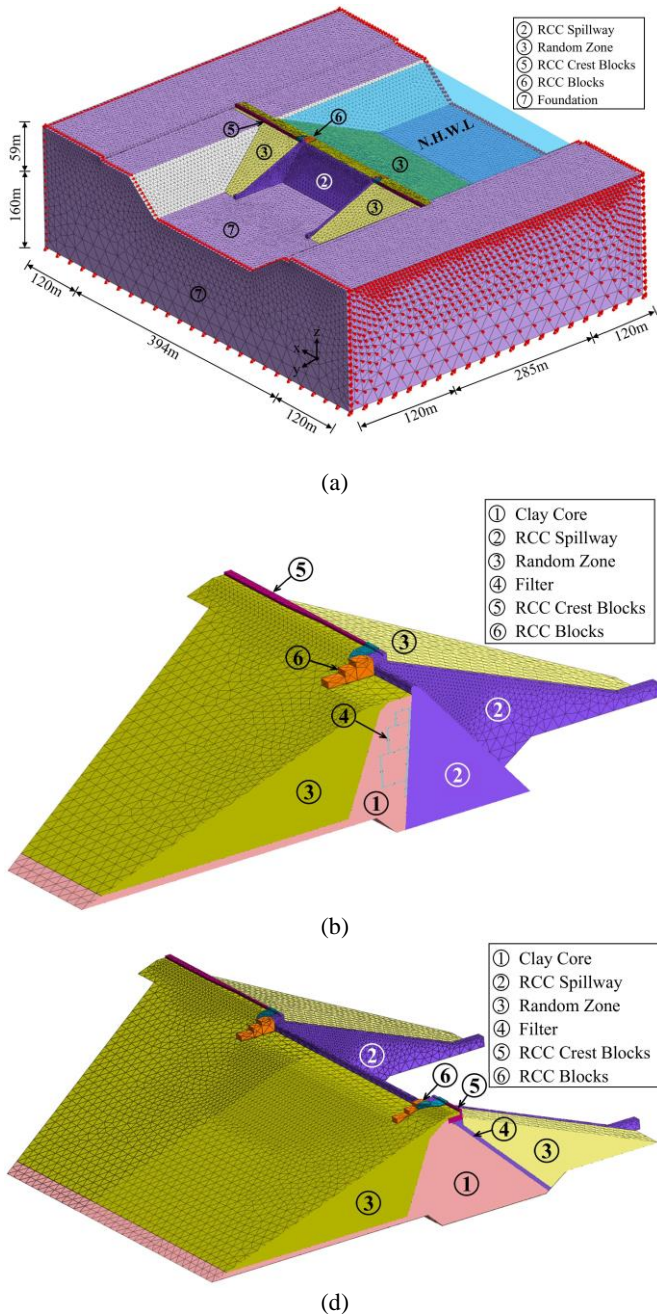


Figure 15 3D Finite Element Model of Mae Suai Dam : (a) 3D Finite Element Model; (b) RCC Spillway section; (c) Earth dam section

4.3 Geotechnical Parameters of the Materials

Some rudimentary information concerning the material parameters used in the analyses were taken from Final design report of Mae Suai Dam (RID, 1998). The parameters were determined from the results of the geotechnical tests done on the samples from the borrow areas, which have been identified during the geological survey of the site, consisting of Identification, Atterberg Limits and Graduation tests, Permeability and Dispersion tests, Proctor test, Direct shear test, and Triaxial Compression Tests. The modulus of elasticity was obtained from finite element back-analysis by assuming the Poisson's ratio (Bergado et al., 1995). The compression index C_c and recompression index C_s used in Modified Cam-clay model are obtained from liquid limit and plastic limit (Alptekin and Taga, 2019). Since the interface layer was defined between the clay core and RCC spillway section, it requires the assumption of simple hypothesis. These elements as

clusters of the model needs to be discretized in 2D mesh elements using the Coulomb friction model. The difficulty of this procedure is to set up the material model for these clusters. In this research, a calculation that was made using this approach on RCC model as a Mohr-Coulomb material. Material properties of RCC was taken from Final design report (RID, 1998), which was determined through the formula proposed by the Spanish regulation EHE-98 (Ardiaca, 2009). 5 different materials used in the 2D, and 3D FE analyses has been presented in Table 1. The Mohr-Coulomb material model was defined for the foundation and filter, while Modified Cam Clay model was used for random and core material.

5. FINITE ELEMENT ANALYSIS RESULTS

2D and 3D finite element analysis results of the Mae Suai Dam are presented in detail in this section. Figure 16 showed the pore pressure head obtained from the transient seepage analysis of 2D and 3D FEM with the water level on the upstream side being +474.00 m. (MSL) and +507.00 m. (MSL) respectively, the pore pressure head was changed for each stage with a difference water level. The characteristics and magnitude of vertical displacement obtained from Fully coupled Stress-Seepage analysis at the end of time step (2014) and geodetic monitoring data were slightly different. The vertical displacement contour of 2D finite element analysis of each section of the right bank is shown in Figure 17. FE analysis results show that the settlement of earth dam is directly proportional to its height. Likewise, RCC spillway section consists of earth dam at the upstream section and RCC at its downstream section. The observed settlement at earth dam is greater than RCC section causing the rotation of RCC block. The rotation has separated block A and RCC spillway as shown in Figure 10. Similarly, the vertical displacement and deformation of 3D FE analysis are shown in Figure 18a. Figure 18b shows the vertical displacement and deformation along the earth dam crest at the left bank; it can be seen that the settlement of the earth dam increases with the height of dam, which is in accordance with the results obtained from the 2D FEM analysis. However, the settlement decreased as it approached the contact area between the earth dam section and the spillway section, which in accordance with the observed data. Figure 18c shows the vertical displacement contour of the earth dam section, which was similar to the 2D FE analysis.

The magnitude of settlement in the model was measured at the position corresponding to the position of the SM. Vertical displacement results along the dam crest (right bank) from FEM analysis were compared with the geodetic monitoring data, as shown in Figure 19. It can be observed that 2D FEM analysis results were slightly higher than to geodetic monitoring data in 2014, while the results of the 3D FEM analysis were slightly less in both cases, approximately 0.24% of the height. However, the trend of result obtained from 3D analysis were similar to that of measurement and observation, i.e., the settlement increases with the height of dam and decreases as it approaches the contact area between the earth dam section and the spillway section. The vertical displacement and deformation of RCC blocks on the right side of the dam from FE analysis, geodetic monitoring data, and site observation showed a similar trend as shown in Figure 5, Figure 10, Figure 11 & Figure 21. Figure 20a & b show the time history of vertical displacement of SM3 and SM4, respectively, 2D and 3D FEM analysis result in each time step (12 years) were compared with the geodetic monitoring data; the analysis results were very close to geodetic monitoring data. The 2D FEM analysis results of SM3 were slightly higher than geodetic monitoring data in the first 2 years and were similar over time. Likewise, 3D FEA was close to geodetic monitoring data in the first 2 years and smaller over time. The 2D and 3D FEM analysis of SM4 was higher than geodetic monitoring data in the first 3 years and were similar over time. However, the characteristics of vertical displacement obtained from FEA and geodetic monitoring data were similar; the rate of settlement was high in the first 2 years and had gradually decreased as the expanded cracks were repaired over time.

Table 1 Material properties used in FEM analyses

Name	Clay Core	Random Zone	Filter	Foundation	RCC
Model Type	Modified Cam Clay	Modified Cam Clay	Mohr Coulomb	Mohr Coulomb	Mohr Coulomb
Elastic Modulus, E (ton/m ²)	3,000.00	3,000.00	5,000.00	300,000.00	1,000,000.00
Poisson's Ratio (ν)	0.30	0.30	0.30	0.20	0.20
Unit Weight γ (ton/m ³)	2.02	2.02	1.85	1.94	2.40
Kx, Ky (m/sec)	2.0x10 ⁻⁷	2.0x10 ⁻⁶	1.0x10 ⁻⁴	3.0x10 ⁻⁷	1.0x10 ⁻⁷
Kz (m/sec)	5.0x10 ⁻⁸	1.0x10 ⁻⁶	1.0x10 ⁻⁴	3.0x10 ⁻⁷	1.0x10 ⁻⁷
Cohesion (ton/m ²)	-	-	-	50.00	30.00
Frictional Angle, φ (Deg.)	-	-	35	40	40
Over Consolidation Ratio, OCR	1.000	1	-	-	-
Slope of NCL, λ	0.335	0.761	-	-	-
Slope of URL, κ	0.053	0.096	-	-	-
Slope of critical state line, M	0.856	1.02	-	-	-

Table note: NCL = normal consolidation line, URL = Unload-reloading line (Overconsolidation line)

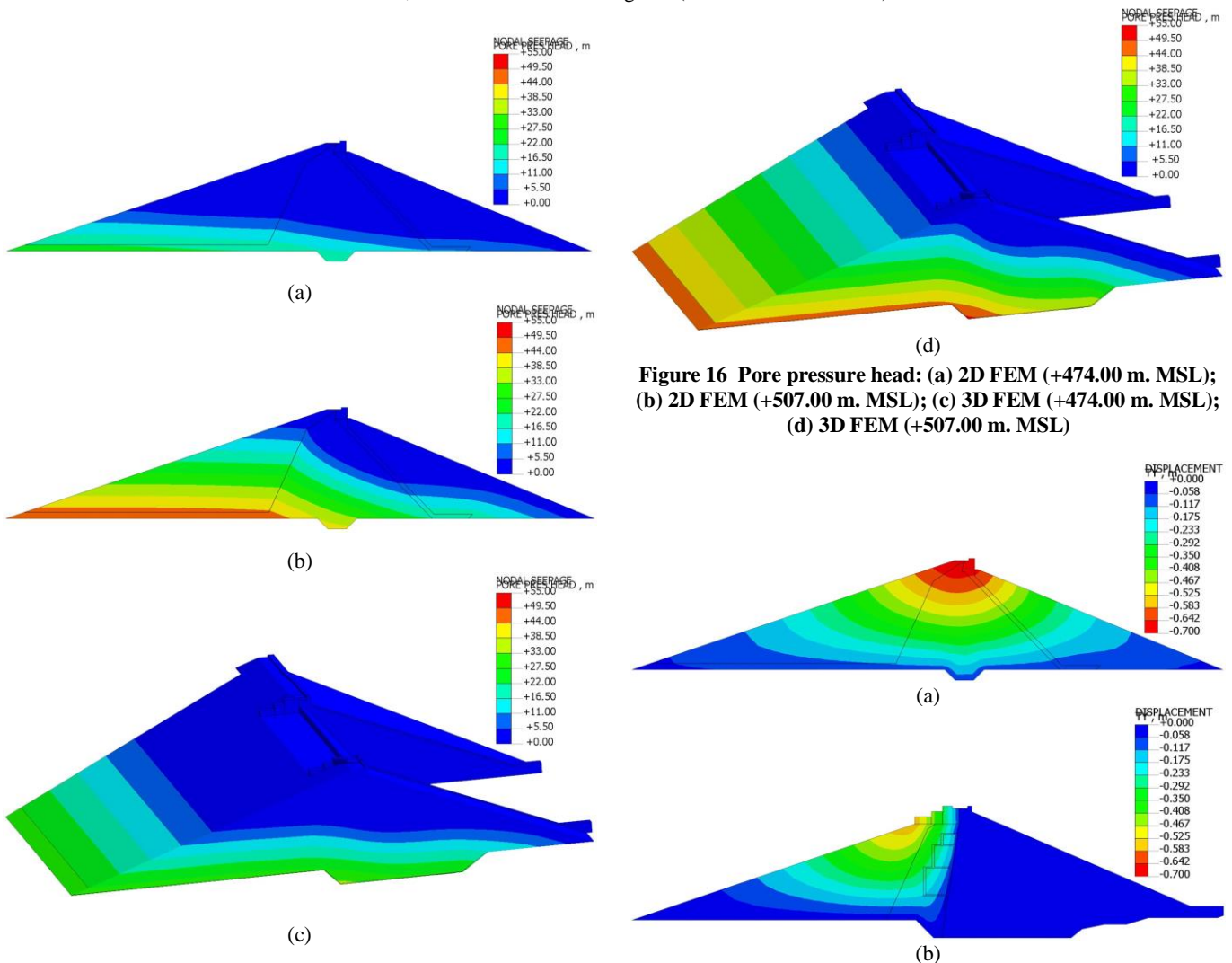


Figure 16 Pore pressure head: (a) 2D FEM (+474.00 m. MSL); (b) 2D FEM (+507.00 m. MSL); (c) 3D FEM (+474.00 m. MSL); (d) 3D FEM (+507.00 m. MSL)

Figure 17 Vertical displacement contour and deformation of 2D Finite Element Analysis: (a) 57.50 m. high (Earth Dam Section); (b) 59.00 m. high (Spillway Section)

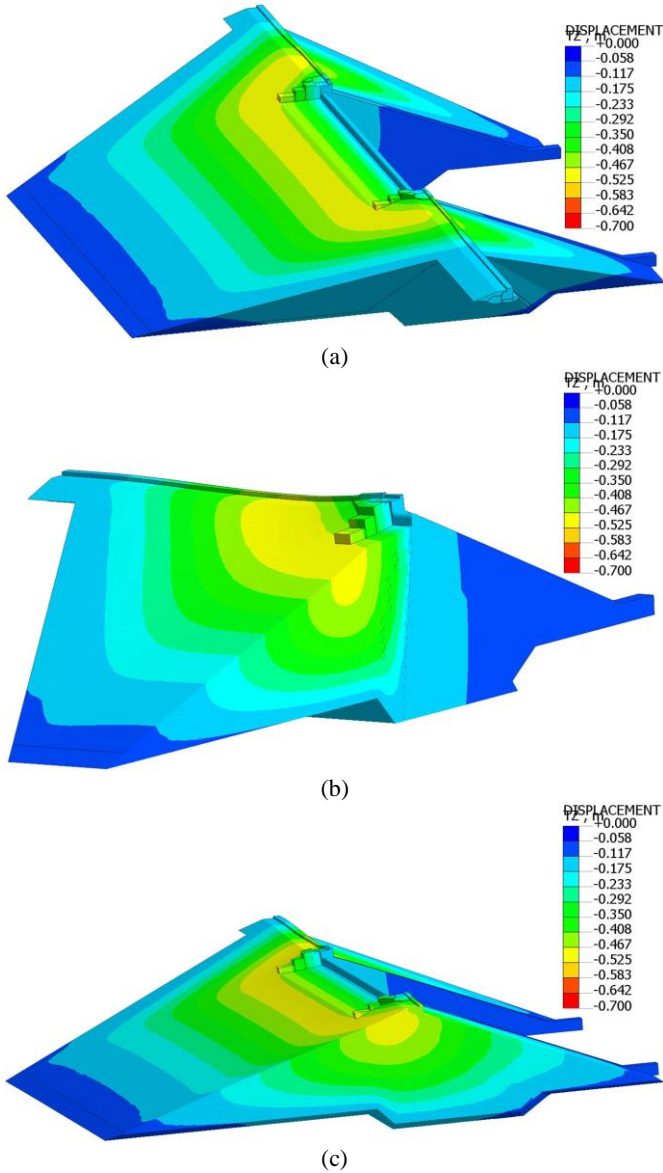


Figure 18 Vertical displacement contour and deformation of 3D Finite Element Analysis: (a) 3D finite element analysis; (b) RCC Spillway section; (c) Earth dam section

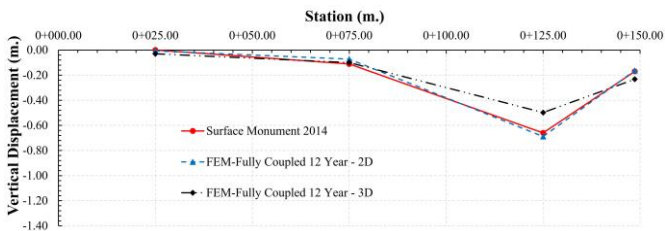


Figure 19 Vertical Displacement result along dam crest (m.)

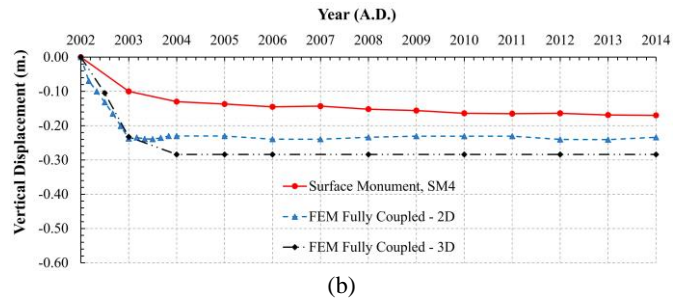
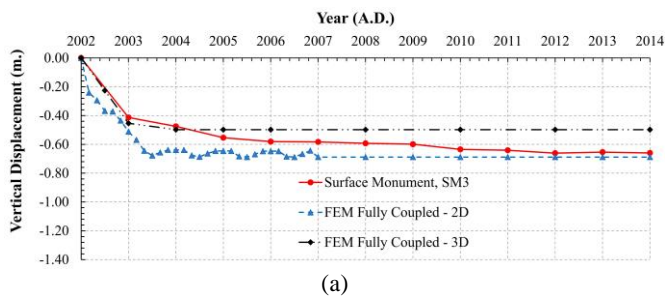


Figure 20 Time history of vertical displacement since the end of construction (2003) to 2014 (m.): (a) SM3; (b) SM4

6. EFFECT OF NON-UNIFORM SETTLEMENT

The results obtained from geodetic monitoring data, site observation, and finite element analysis represents uneven settlement in two parts, i.e., 1) the contact area between the RCC block D overlaid on the earth dam and spillway section along the dam crest. 2) The contact area between RCC block A, i.e., wing wall and spillway section on upstream side. The assumption on the roughness and taper effect causing a non-uniform settlement was examined from physical observations in rehabilitation processes. The analysis of settlement along dam crest showed that the settlement of the earth dam increases with height of embankment and decreases as it approaches the contact area between the earth dam section and spillway section. RCC Block A attached to the spillway section, is rotated due to the taper and roughness effect (Figure 21). The side adjacent to the spillway had the lowest settlement and had increased as it moved further away. The separation of RCC block A and spillway section in FE analysis corresponded with the geodetic monitoring data (Figure 10) and field observation (Figure 11). The deformation of the RCC block and rotation of Block D from 2D & 3D Finite element analysis is shown in Figure 18b & Figure 21. Likewise, the side adjacent to spillway had the lowest settlement and increased as it moved further away.

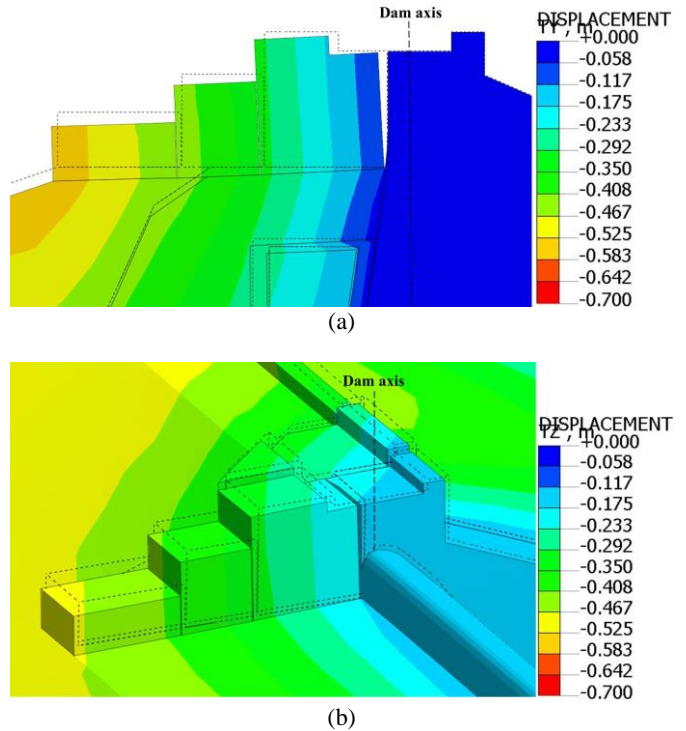


Figure 21 Vertical displacement contour and deformation of RCC Block A, B, C & D; (a) 2D Finite Element Analysis; (b) 3D Finite Element Analysis

Furthermore, characteristics of settlement and tendency of the maximum shear stress were examined from physical observations and finite element analysis during the rehabilitation processes. The design of RCC crest block is as shown in Figure 22. It can be seen that the designer had an intention to deal with future differential settlement by making the crest elevation of earth dam section higher than the RCC section, in other words adding the camber. The results from finite element analysis showed that RCC block D had maximum shear stress and was greater than the shear strength of RCC (Figure 25). The characteristics of the settlement and occurrence of the crack in contact area between earth dam section and spillway section during the rehabilitation corresponded with the results of finite element analysis as shown in Figure 23 & Figure 24. The figure also shows the upward tilting of RCC block D due to shear cracking, i.e., the block was raised higher than the adjacent spillway section due to shear cracking (Figure 7 & Figure 8). The cracks observed at the RCC block D (Figure 24) are consistent with the results obtained from finite element analysis (Figure 25), causing leakage through RCC material to downstream section of the dam. The result from geodetic monitoring data and FEA shows the increase in settlement over time, especially during the first five years. After repairing the dam in 2004, the crack gradually expanded with the passage of time, leading to the significant increase in the rate of leakage.

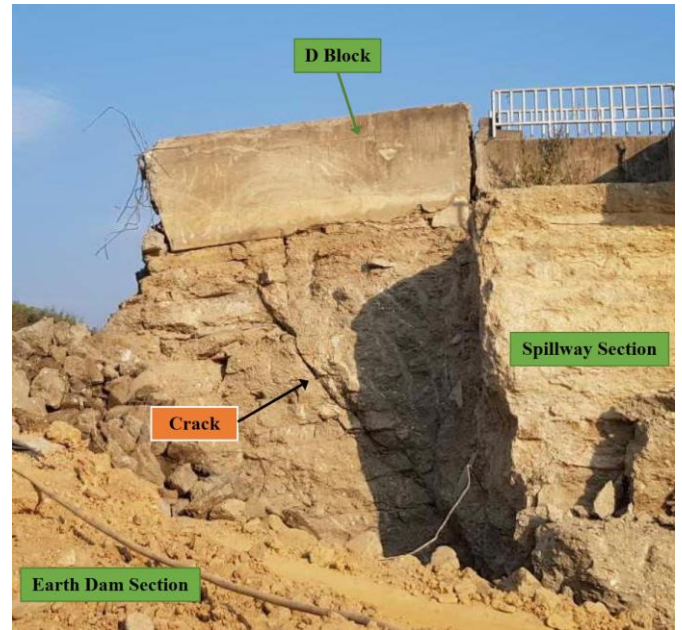


Figure 24 Crack appeared in the rehabilitation processes of Mae Suai Dam (2019)

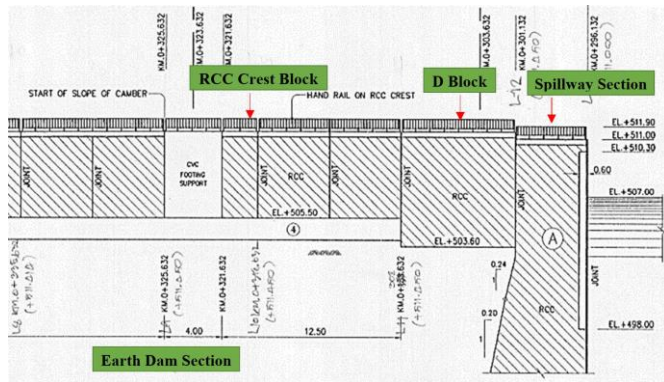


Figure 22 RCC crest block (RID, 1998)

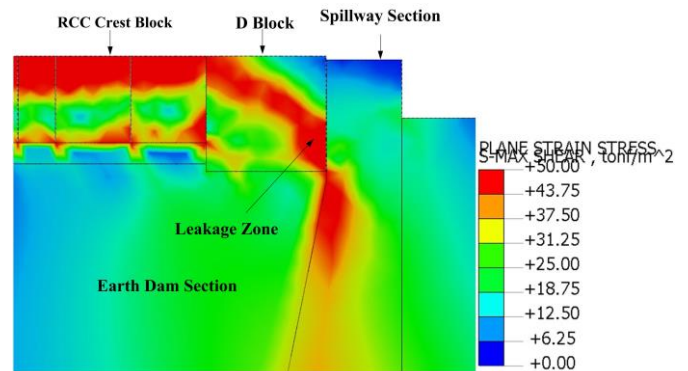


Figure 25 Maximum Shear Stress, 2D Finite Element Analysis of Mae Suai Dam



Figure 23 Rehabilitation processes of Mae Suai Dam (2019)

7. ROUGHNESS AND TAPER EFFECT

The estimated settlement of the earth dam in Final design report of Mae Suai Dam was based on dam’s height, i.e., 1% of dam height. The maximum estimated settlement was 43cm, and the settlement pattern was predicted, as shown in Figure 21. The sufficient camber of 45cm was provided to accommodate the settlement by increasing the level of blocks A, D, and RCC crest block. However, the actual dam settlement pattern was non-uniform, as shown in Figure 22, which was confirmed by the results of geodetic monitoring data and was consistent with the results obtained from 2D and 3D FEM analysis. Roughness and taper effects were presumed to be the cause of non-uniform settlement. Xiaobin Chen and his co-workers examined the effect of surface roughness on red clay-concrete interfaces by laboratory using large-scale direct shear tests for different types of red clay-concrete interfaces (Chen et al., 2015). The surface roughness was found to have an effect on the interfacial shear strength and shear behavior, i.e., surface roughness increased with increase in shear strength. The effects of taper and roughness were studied by analyzing the settlement along the dam crest using 2D FEM analysis.

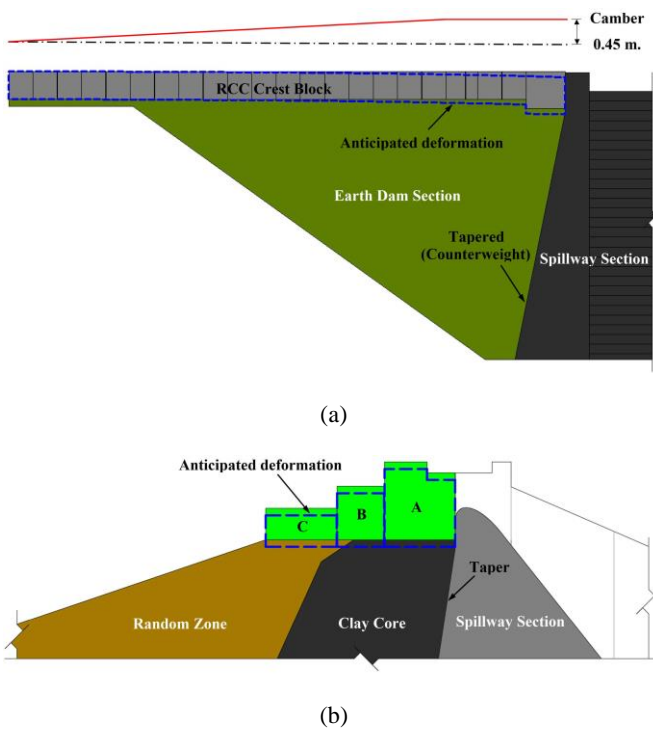


Figure 26 Anticipated settlement of Mae Suai Dam : (a) Longitudinal Settlement; (b) Transverse Settlement

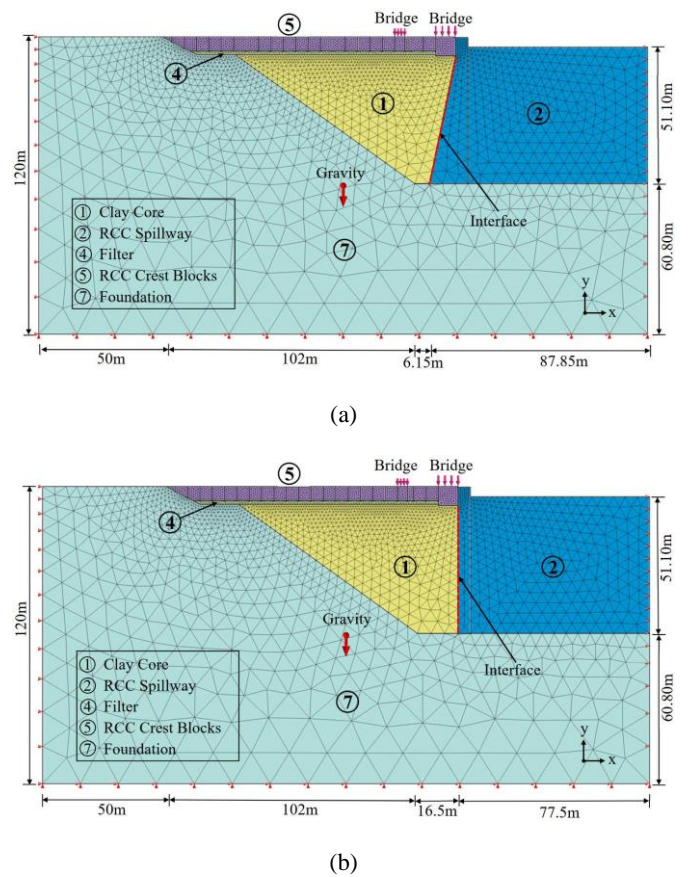


Figure 28 2D Finite Element Model Along the dam crest: (a) Taper effect; (b) Non-Taper effect

Figure 28 shows a longitudinal 2D FEM of the dam considering the effect of the taper and non-taper, respectively. In each case, the interface layer was defined between the clay core and spillway section. The shear strength of the clay-RCC interface was decreased by using Strength Reduction Factor (R_{inter}) that is directly related to the shear strength of clay (Equation 10); G_i = the shear module of interface, G_{soil} = shear modulus of soil by $R_{inter} = 1.00, 0.75, 0.50$ and 0.10 to study the characteristics of the longitudinal settlement of the dam.

$$G_i = R_{inter} \cdot G_{soil} \quad (10)$$

Figure 29 shows the vertical displacement contour and deformation along the dam crest with taper effect. In case of the smooth interface, $R_{inter} = 0.10$ (Figure 29a), the settlement of the clay core will slide along the inclination of the RCC spillway, and the highest settlement will be located at the contact between the clay and the RCC spillway. The pattern of settlement corresponded with the anticipated settlement (Figure 26a). Likewise, when the interface stiffness of the contact was increased ($R_{inter} = 0.5, 0.75$), it resulted in less settlement at the contact area (Figure 29b and Figure 29c). Furthermore, in case of the interface stiffness was high or equal to clay, $R_{inter} = 1.00$ (Figure 29d), it resulted in very less settlement at the contact area. The maximum settlement was further away from the contact area, and the pattern of settlement corresponded with the geodetic monitoring data, observation, and 3D FEM analysis. Therefore, the analysis showed that the settlement in the contact area decreases with an increase in interface stiffness.

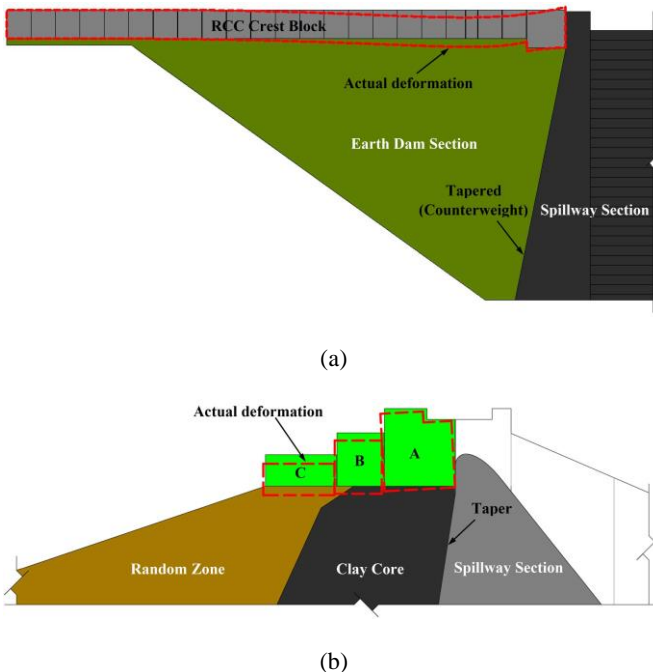


Figure 27 Actual settlement of Mae Suai Dam : (a) Longitudinal Settlement; (b) Transverse Settlement

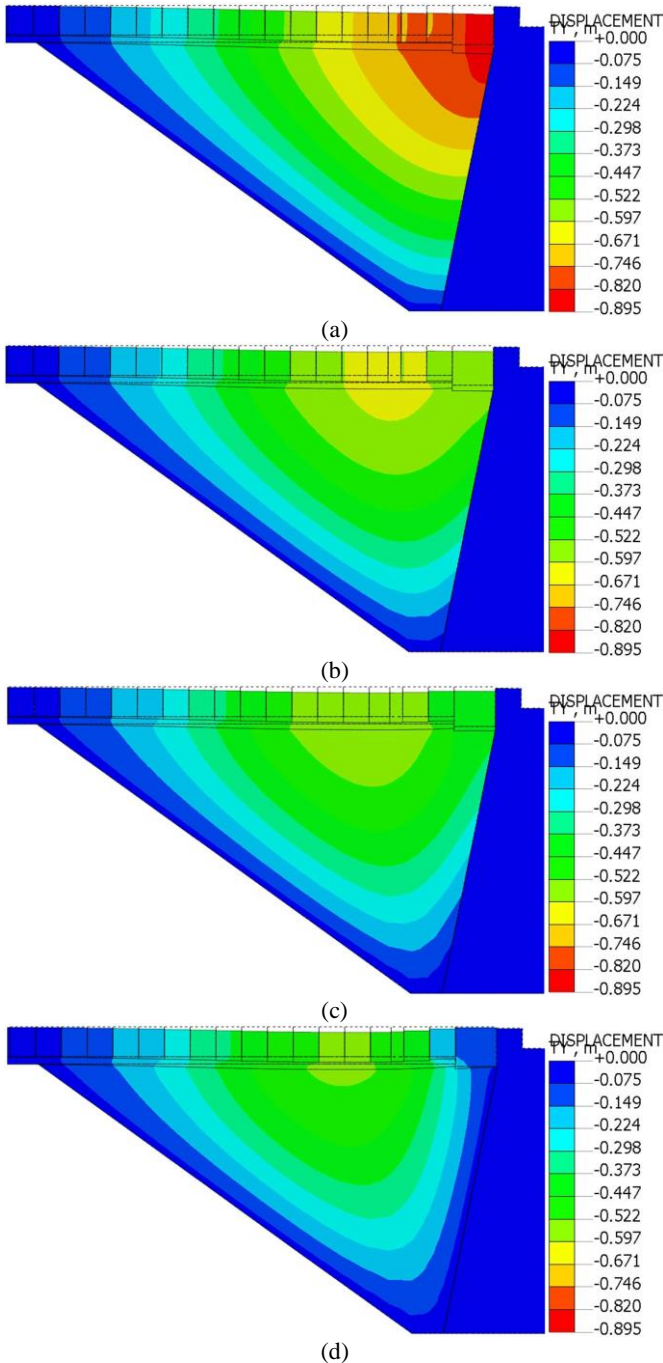


Figure 29 Vertical displacement contour and deformation along the dam crest of 2D Finite Element Analysis, taper effect: (a) $R_{inter} = 0.10$; (b) $R_{inter} = 0.50$; (c) $R_{inter} = 0.75$; (d) $R_{inter} = 1.00$

Figure 30 shows the vertical displacement contour and deformation along the dam crest without consideration of taper effect; the contact of clay and RCC spillway was vertical. In case of the smooth interface, $R_{inter} = 0.10$ (Figure 30a), the maximum settlement was observed at the contact between clay and RCC spillway; the pattern of settlement corresponds to the anticipated settlement as in case of considering the taper effect with smooth interface (Figure 26a). Figure 30b & c shows the settlement where the interface stiffness was increased ($R_{inter} = 0.5, 0.75$), the settlement at the contact was decreased, and settlement pattern remains consistent with the anticipated settlement. Furthermore, in case of the interface stiffness was high or equal to the clay core, $R_{inter} = 1.00$ (Figure 30d), the contact area had very less settlement, and the settlement pattern began to change. The maximum settlement was further away from the contact area; the pattern of settlement corresponds to the actual settlement as in case of considering the taper effect.

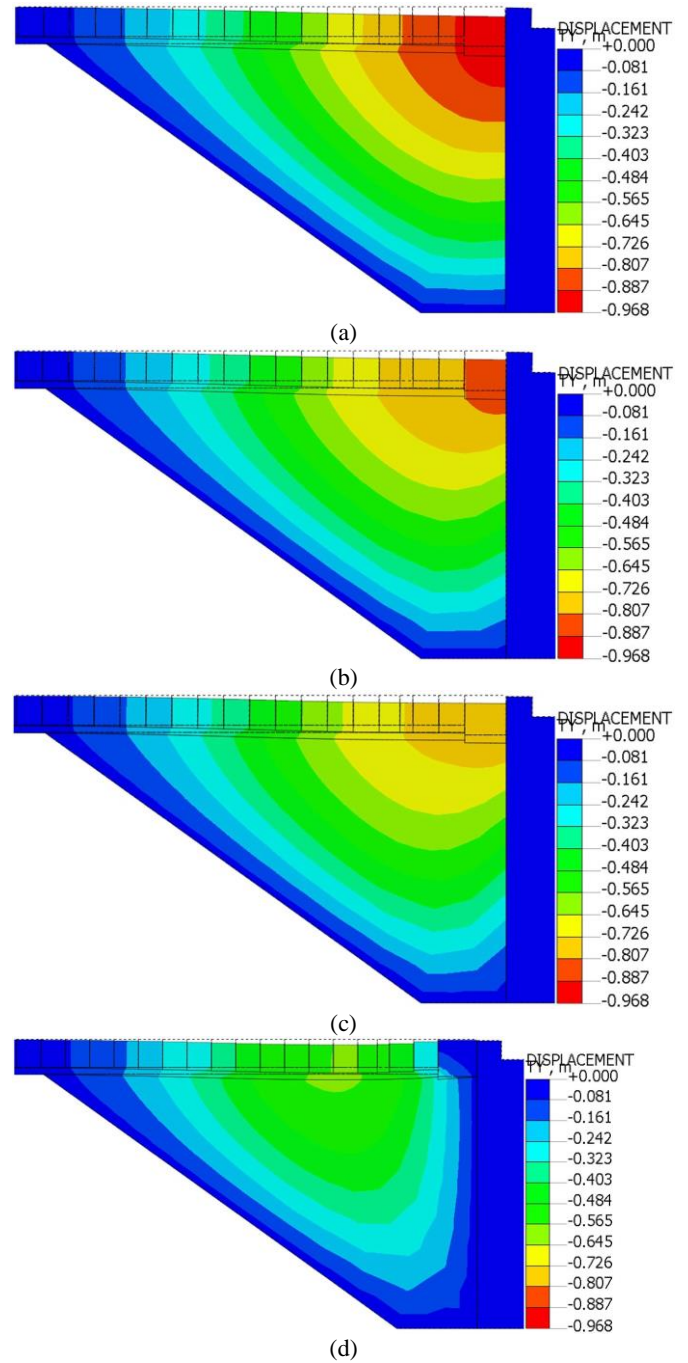


Figure 30 Vertical displacement contour and deformation along the dam crest of 2D Finite Element Analysis, non-taper effect: (a) $R_{inter} = 0.10$; (b) $R_{inter} = 0.50$; (c) $R_{inter} = 0.75$; (d) $R_{inter} = 1.00$

From the analysis, it was found that the interface stiffness was the cause of less settlement of contact area. When the interface stiffness was equal to the clay, the contact area has the roughness of RCC surface, interlocking the texture of RCC with clay surface. The clay at the contact was not able to slide down along RCC inclination, and therefore there was small differential settlement between the two parts of contact area. This roughness of the RCC surface was observed during the rehabilitation of the dam as shown in Figure 31. The roughness during the construction was obtained by either compacting the RCC and each layer of clay together or using a material as a formwork with another material (Figure 32). Likewise, the taper of the RCC spillway causes the clay at the contact to be compacted with higher interface stiffness; this can be observed from the case of $R_{inter} = 0.5, 0.75$ that does not consider the taper effect, the settlement pattern remains consistent with the anticipated settlement and began change when $R_{inter} = 1.00$. It shows that when taper effect

is not considered, the interface strength must be higher than the case where taper effect is considered because the clay at the contact could slide down. Therefore, the effects of both roughness and taper have significant effect on non-uniform settlement.



Figure 31 Roughness Surface in rehabilitation processes of Mae Suai Dam (2019)

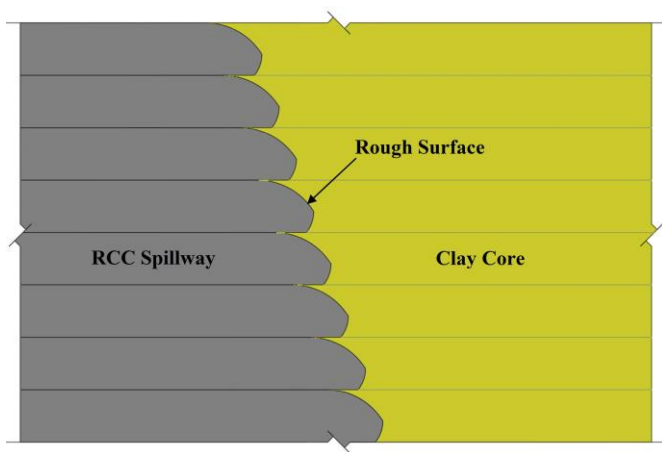


Figure 32 Rough surface between RCC spillway and clay core

8. DISCUSSIONS AND CONCLUSIONS

In this paper, the settlement pattern of Mae Suai Dam was investigated by 2D and 3D FEM using MIDAS GTS for Fully coupled Stress-seepage analyses. The results were verified with the geodetic measurements data and field observation in rehabilitation processes. 2D FEM analysis results were slightly higher than to geodetic monitoring data in 2014, while the results of the 3D FEM analysis were slightly less in both cases, possibly because of the three 3D loading conditions and geometric effects which are significant influence factors on numerical simulation (Auvinet and Gonzalez, 2000) and the foundation of the earth dam was trapezoidal in shape and the settlement of the earth dam confined with abutment and RCC Spillway that corresponded to the actual structural conditions, while 2D FEM analysis is a plain strain analysis. Therefore, the settlement of 3D analysis and geodetic monitoring data was less than FEM 2D analysis. However, the aim of this research was to study the differential settlement between earth dam and RCC section that causes unusual settlement pattern in which the FE analysis result was consistent with geodetic monitoring data and field observation. The actual settlement pattern of dam is as shown in Figure 22 and has been divided into 2 parts:

1. The longitudinal settlement: The contact area has very less settlement, the maximum settlement was far from the contact area and

decreases gradually as it moved near the abutment, causing block D to rotate, and the cracks were observed due to shear stress.

2. The transverse settlement: It was observed especially at the position of the wing wall (Block A, B&C), the contact area has very less settlement and increased as it moved further away, causing the block A to rotate and the cracks were observed at the contact between block A and RCC spillway.

Therefore, it can be concluded that leakage was observed in RCC block D through the cracks between the block A and RCC spillway, or water passing through the internal cracks of block A and in front of block D and leaked to downstream through the cracks in the contact area. Over time, more and more settlement was observed causing the cracks to expand and increased leakage even after repairing in 2005. Designer had predicted the dam settlement pattern and provided the camber to accommodate the settlement by increasing the level of the block D, A, and RCC crest block near the contact area. In reality, the pattern of settlement was non-uniform, and settlement in the contact area was less. The analysis revealed that the effect of roughness and taper resulted in non-uniform settlement as the clay at contact area was not able to slide down along the RCC inclination.

This roughness was caused by the construction process by either compacting the RCC and each layer of clay together or using a material as a formwork with another material. However, the taper causes the clay at the contact to be compacted which leads to the increase in interface stiffness. Therefore, both roughness and taper have the effect on non-uniform settlement. The interaction between clay-concrete interface with roughness is useful for potential engineering applications, such as deep foundations or high composite dams. The shear resistance from roughness at interface used in the finite element analysis should be close to the strength of the clay ($R_{inter} = 1.00$) for determining the actual behavior of settlement. However, during the construction process, it is difficult to smoothen the RCC surface and allow the earth dam to slide down along the RCC inclination. The taper is also necessary to prevent the seepage through the contact between clay and RCC spillway.

If these types of dam structures are selected in other projects, the pattern of settlement should be considered in accordance with the guidelines for dam crest design to prevent damage and leakage caused by the non-uniform settlement of the dam. RCC block as the dam crest should be placed above the maximum water level of the dam to reduce the leakage at the downstream side. Additionally, to reduce the effect of roughness at the interface, CVC curb should be used instead of direct soil-to-RCC collision compaction.

9. ACKNOWLEDGMENTS

Acknowledgments are encouraged as a way to thank those who have contributed to the research or project but did not merit being listed as an author. Authors can include an acknowledgment section to recognize any advisory or financial help received.

10. REFERENCES

- Alidadi, S. and Hakami, M. (2014). "Rehabilitation of Temporary Composite Dams (Case Study: Mared Soil-Sheet Pile Dam)." *Geotechnical and Geological Engineering*, 33, 137-142.
- Alptekin, A. and Taga, H. (2019). "Prediction of Compression and Swelling Index Parameters of Quaternary Sediments from Index Tests at Mersin District." *Open Geosciences*, 11, 482-491.
- Ardiaca, D. H. (2009). "Mohr-Coulomb Parameters for Modelling of Concrete Structures [Online]." [Accessed].
- Auvinet, G. and Gonzalez, J. L., (2000). "Three-Dimensional Reliability Analysis of Earth Slopes." *Computers and Geotechnics* 26, 247-261.
- Bergado, D.T., Chai, J.C., and Miura, N. (1995). "FE Analysis of Grid Reinforced Embankment System on Soft Bangkok Clay." *Computers and Geotechnics*, 17: 447-471.
- Borja, R. I. (1989). "Cam Clay Plasticity, Part II: Implicit Integration of Constitutive Equation Based on a Nonlinear Elastic Stress Predictor." *Computer Methods in Applied Mechanics and Engineering*, 225-240.

- Chang, N. Y. and Oncul, F. A. (2000). "Parametric Study on Seismic Behavior of a Composite Dam." *Geo-Denver 2000 Denver, Colorado, United States*.
- Chen, Q. and Zhang, L. M. (2006). "Three-Dimensional Analysis of Water Infiltration into the Gouhou Rockfill Dam Using Saturated–Unsaturated Seepage Theory." *Canadian Geotechnical Journal*, 43, 449-461.
- Chen, X., Zhang, J., Xiao, Y., and Li, J. (2015). "Effect of Roughness on Shear Behavior of Red Clay – Concrete Interface in Large Scale Direct Shear Tests." *Canadian Geotechnical Journal*, 52, 1122-1135.
- Dong-Soo, K. (2018). "Numerical Modeling on Seismic Behaviors of Two Different Composite Dams Twenty-Sixth International Congress on Large Dams." 4th-6th July, Vienna, Austria.
- Farias, M. M. D. and Cordão Neto, M. P. (2010). "Advanced Numerical Simulation of Collapsible Earth Dams." *Canadian Geotechnical Journal*, 47, 1351-1364.
- Foster, M., Fell, R. and Spannagle, M. (2000). "The Statistics of Embankment Dam Failures and Accidents." *Canadian Geotechnical Journal*, 37, 1000-1024.
- Gikas, V. and Sakellariou, M. (2008). "Settlement analysis of the Mornos Earth Dam (Greece): Evidence from Numerical Modeling and Geodetic Monitoring." *Engineering Structures*, 30, 3074-3081.
- Jia, Y., Xu, B., Chi, S., Xiang, B., Xiao, D., and Zhou, Y. (2018). "Joint Back Analysis of the Creep Deformation and Wetting Deformation Parameters of Soil Used in the Guanyinyan Composite Dam." *Computers and Geotechnics*, 96, 167-177.
- Kartal, M. E., Çavuşlı, M., and Genç, M. (2019). "3D Nonlinear Analysis of Atatürk Clay Core Rockfill Dam Considering Settlement Monitoring." *International Journal of Geomechanics*, 19.
- Kermani, M., Konrad, J. M., and Smith, M. (2016). "An Empirical Method for Predicting Post-Construction Settlement of Concrete Face Rockfill Dams." *Canadian Geotechnical Journal*, 54, 755-767.
- Lollino, P., Cotecchia, F., Zdravkovic, L., and Potts, D. M. (2005). "Numerical Analysis and Monitoring of Pappadai Dam." *Canadian Geotechnical Journal*, 42, 1631-1643.
- Luo, J., Zhang, Q., Li, L., and Xiang, W. (2019). "Monitoring and Characterizing the Deformation of an Earth Dam in Guangxi Province, China." *Engineering Geology*, 248, 50-60.
- Mahinroosta, R., Alizadeh, A., and Gatmiri, B. (2015). "Simulation of Collapse Settlement of First Filling in a High Rockfill Dam." *Engineering Geology*, 187, 32-44.
- Midasgts (2018). "Midas GTS Reference Guide (Part 1, Part 2, Part 3 & Part 4)." https://en.midasuser.com/training/technical_list.asp?nCat=267.
- Panthi, K. and Soralump, S. (2020). "Estimation of Failure Surface of Pa Bon Dam from Site Investigation." *Jordan Journal of Civil Engineering*, 14, 97-107.
- Pérez-González, E., Bilodeau, J. P., Doré, G., and Doré-Richard, S. (2020). "Assessment of the Permanent Deformation at the Earth Core of a Rockfill Dam Under Heavy Vehicle Loading." *Canadian Geotechnical Journal*, 58, 165-175.
- Rashidi, M. and Haeri, S. M. (2017). "Evaluation of Behaviors of Earth and Rockfill Dams during Construction and Initial Impounding Using Instrumentation Data and Numerical Modeling." *Journal of Rock Mechanics and Geotechnical Engineering*, 9, 709-725.
- RID. (1998). "Design Criteria: Mai Suai Dam Project."
- Saberi, M., Annan, C. D. and Konrad, J. M. (2018). "Numerical Analysis of Concrete Faced Rockfill Dams Considering the Effect of Face Slab-Cushion Layer Interaction." *Canadian Geotechnical Journal*, 55, 1489-1501.
- Soralump, S., Panthi, K., and Prempramote, S. (2021a). "Assessment of the Upstream Slope Failure of a Dam Due to Repeated Cyclic Drawdown." *Soils and Foundations*, 61, 1386-1398.
- Soralump, S., Pien-Wej, N., Panthi, K., and Sanmuang, J. (2019). "Cyclic Drawdown of Water Causing the Slope Failure of Canal and Dam." *16th Asian Regional Conference on Soil Mechanics and Geotechnical Engineering*, October 14-18, Taipei, Taiwan.
- Soralump, S., Shrestha, A., Jotisankasa, A., Thongthamchart, C., and Isaroran, R. (2021b). "Use of Geosynthetic Clay Liner as a Remedial Measure of Claystone Degradation in Lam Ta Khong Hydropower Plant." *Geotextiles and Geomembranes*, 49, 1211-1228.
- Soralump, S., Thongthamchart, C., and Chaisakaew, V. (2009). "30 Years Instrumentation Behavior of Srinagarind Dam and Analysis of Warning Criteria." *Long Term Behaviour of Dams*, 871-876.
- Soralump, S., Thongthamchart, C., Jinagoolwipat, M., and Boonpo, A. (2016). "Rehabilitation of Leakage and Seismic Damaged Problem of Mae Suai Earth Zone Composited RCC Dam." *19th Southeast Asian Geotechnical Conference*, Kuala Lumpur, Malaysia.
- USBR. (2011). "Design Standards No. 13 Embankment Dams (Chapter 4: Static Stability Analysis Phase 4)." U.S. Department of the Interior Bureau of Reclamation.
- Wang, Y., Liu, X., Zhang, M., Bai, X., and Cavaleri, L. (2020). "Effect of Roughness on Shear Characteristics of the Interface between Silty Clay and Concrete." *Advances in Civil Engineering*, 2020, 1-9.